Rafidain Journal of Science

https://rsci.uomosul.edu.iq

Vol. 35, No. 1, pp. 119-127, 2026 (March)

Preparation of Zinc Selenide (ZnSe) Nanoparticles by Chemical bath deposition, Study the Surface Morphology and Optical Properties

Alaa A. Mahmood **Suha A. Najim**

Department of Physics/ College of Science/ University of Mosul

p-ISSN: 1608-9391
e -ISSN: 2664-2786

Article information

Received: 3/7/2025
Revised: 25/8/2025
Accepted: 7/9/2025

DOI: 10.33899/rsci.v35i1.62001

corresponding author:
Suha A. Najim
suhaabdullah@uomosul.edu.iq

ABSTRACT

Zinc Selenide thin films were deposited on a glass substrate by chemical bath deposition. The optical properties and annealing temperature at 250°C for 1 hour were observed, the results showed an increase in transmittance and an increase in the band gap after annealing. They were analyzed by XRD and revealed a polycrystalline structure; the results indicated that the samples exhibited a mixture of cubic and hexagonal structures. After annealing at 250°C, observed an increase in the intensity of the plans, a slight shift in the diffraction angles, and a decrease in the average crystal size. The elemental composition of the Zinc Selenide (ZnSe) films using EDX revealed the presence of other elements such as C, O, Si, S, Ca, Cl, Mg and Na in varying percentage which they indicate the presence of impurities during the preparation process. Field Emission Scanning Electron Microscope observations were performed at different magnifications (15,000, 30,000, 60,000, and 120,000X). Zinc Selenide (ZnSe) nanoparticles were distributed in various sizes (21–35 nm) and exhibited a spherical shape.

Keywords: ZnSe, morphology, optical, nanoparticles, deposition.

INTRODUCTION

Nanoparticles are particles with dimensions ranging from 1 to 100 nanometers, existing in one dimension (Rogach, *et al*., 2008). At this level, nanoparticles change their physical and electronic properties in addition, they improve their mechanical and electrical properties. (Chen *et al*., 2004). Their properties also include controlling electrical conductivity by changing (voltage, absorption, and emission of photons). Zinc selenide is important for its use in many practical applications, including windows, lenses, output comparators, beam expanders, and optically controlled switching, due to its low absorbance at infrared wavelengths, high visible transmittance (Fang *et al*., 2009) (Wang *et al*., 2005) and high light sensitivity (Wang *et al*., 2005). It exists in two structural forms: cubic and hexagonal (Deng *et al*., 2007). Zinc selenide (ZnSe) is of wide interest as a material for optoelectronic devices, including blue lasers, light-emitting diodes (LEDs) (Elsaeedy *et al*., 2021), and photodetectors, due to its wide direct bandgap (2.67 eV) (Gudiksen *et al*., 2001; Wang *et al*., 2010; Soonmin *et al*., 2023).

The study of the structural, morphological, optical and electrical properties of ZnSe thin films is of great importance for their improved application. There are several methods for depositing ZnSe thin films, including thermal evaporation, pulsed laser deposition, electron beam evaporation, molecular beam epitaxy, sol-gel deposition, spray pyrolysis and chemical bath deposition (Wang *et al.,*2010). It is found to be cheap, low deposition temperature and simple way to deposit large area thin film (Kale and Lokhande, 2005; Ezema and Osuji, 2007). In this paper, syntheses ZnSe nanoparticles by CBD then study the optical characteristics' before and after annealing temperature at 250 ◦C and the surface structures by XRD, FESEM and EDX.

PROCEDURES METHOD

Zinc selenide (ZnSe) thin films have been deposited on glass substrates by chemical bath deposition at room temperature. They cleaning using ethanol, distilled water for two minutes and finally dried with an air. Zinc selenide (ZnSe) films are prepared by mixing 0.5 M selenium in 10 ml of distilled water with 0.5 M of sodium sulfide, then we boil the mixture for three hours. The last solution used of the element zinc selenide. Moreover, the mix solution with 0.5 M of ($ZnCl_2$) in 10 ml of distilled water with 1 ml ammonia. The solution is placed over hater and mixing magnet for 1 min., we put the slides inside the solution and leave them in mixture approximately 24 hours, then remove them from the bath and leave them to dry and measure their optical properties using a spectrophotometer and study structural properties by FESEM, XRD and EDX.

RESULTS AND DISCUSSION

UV-Vis Spectrophotometer was used to measure the transmittance spectra. (Fig. 1) shows the variation of transmittance spectra for wavelengths ranging from 300 to 1000 nm. It is noted that a sharp decrease at the band edge in the range of 300-400 nm; they do not appear below this range. The highest value of interference fringe intensity reaches about 86% in the transparent region in infrared, and the Zinc selenide (ZnSe) transmittance increases in the visible range at the wavelength (400-780 nm) and occur the direct electronic transmission in this region (Prakash *et al*., 2016). This value increases slightly after annealing as shown in (Fig. 1 b), which is attributed to improved crystallinity and reduced defects. Annealing reduces the presence of surface defects such as unsaturated bonds or suspended atoms, reduces unwanted internal absorption, and increases transmittance in the visible and infrared spectrum.

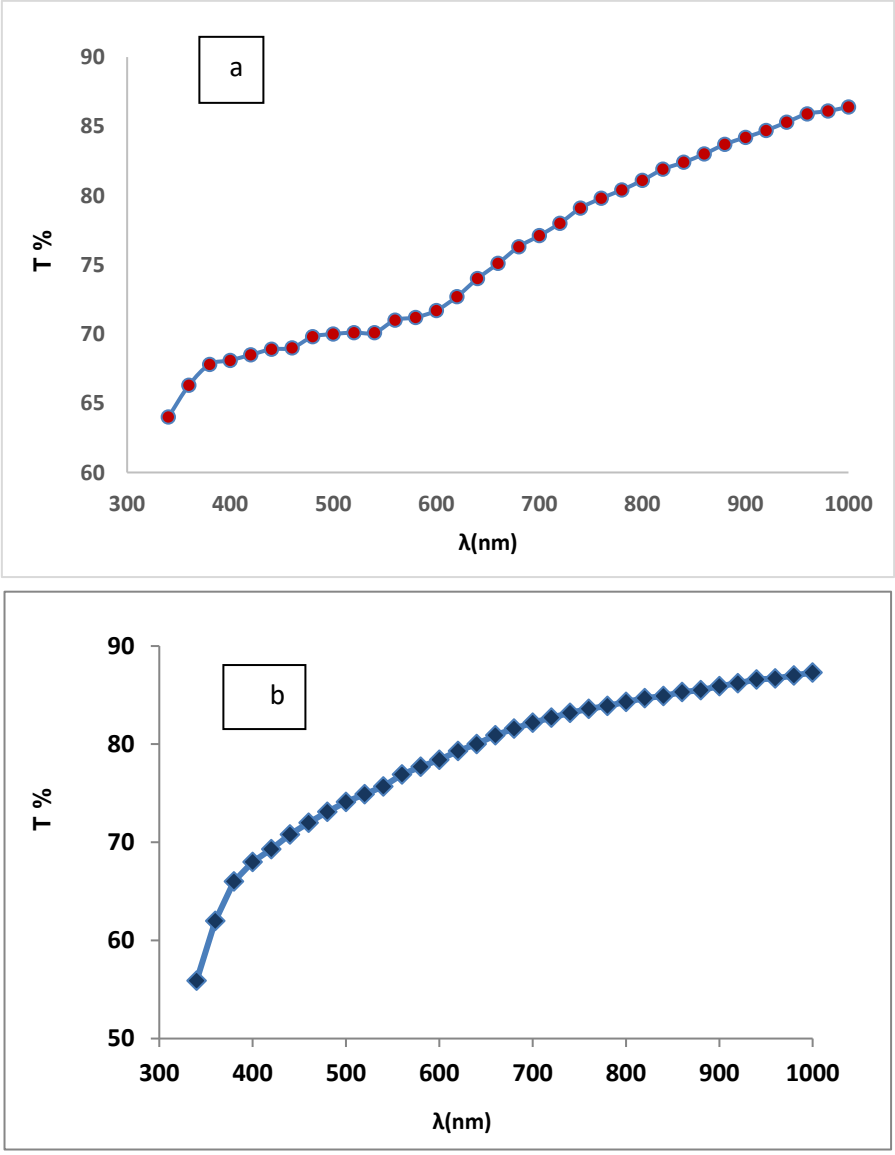

Fig. (1) a: Transmittance vs. wavelength before annealing
b: Transmittance spectra variation with wavelength after annealing

(Fig. 2) and (Fig. 3) shows the energy gap of the Zinc selenide (ZnSe) compound before and after annealing for one hour 250°C. For Zinc selenide (ZnSe) thin film, the optical bandgap energy was estimated as 2.7 eV and this value is equal for bulk Zinc selenide (ZnSe) films as shown in (Fig. 2). After annealing process, the energy gap increases to reach at 2.82 eV in (Fig. 3). This is attributed to the rearrangement of the atoms within the lattice, reducing the gaps and lack of regularity. This in turn leads to the disappearance of levels within the energy gap, which leads to increase in the energy gap (Abou El-Ela *et al*., 2018). The relation between (α) and photon energy is given by Tauc equation (1) (Najim *et al*., 2019).

$$\alpha h\nu = A(h\nu - Eg)^{1/2} \quad \text{----------(1)}$$

h: Plank constant, ν: frequency for incident photon, A: constant and E_g: band gap energy.

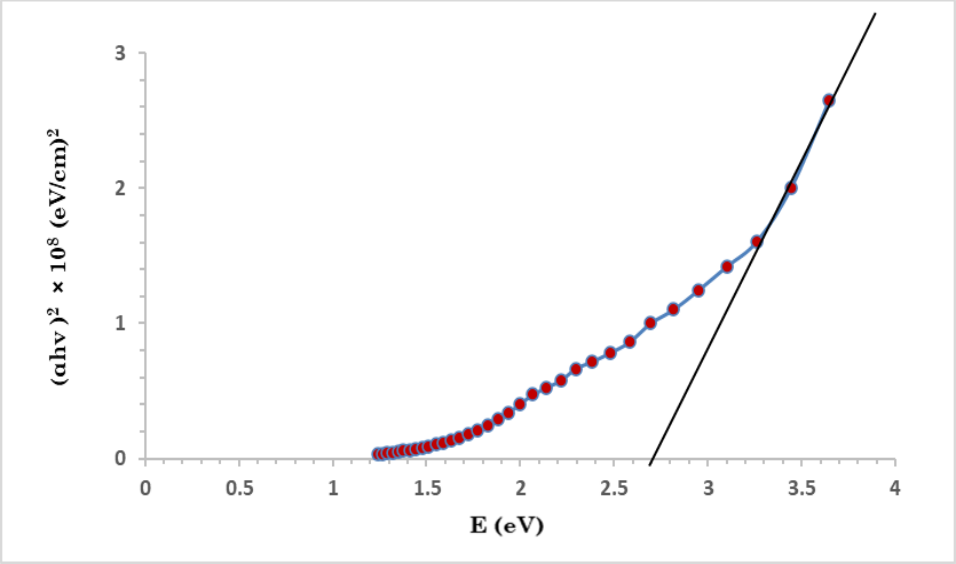

Fig. (2): (αhv)^2 vs. photon energy for Zinc selenide (ZnSe) before annealing

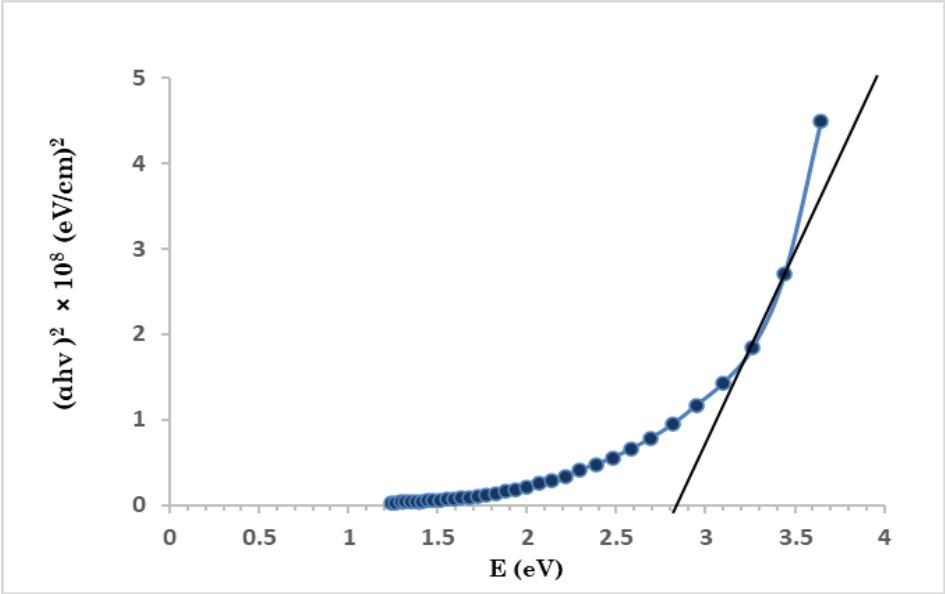

Fig. (3): (αhv)^2 vs. (E) for Zinc selenide (ZnSe) after annealing

An X-ray Diffractometer was used. (Fig. 4) shows the X-ray diffraction analysis of the synthesized ZnSe nanoparticle samples, which is listed in Table (1). The samples exhibited polycrystalline behavior, and the peaks appeared to be sharper, which could be identified by the intense (200) peak and the other planes (220), (400), (311), and (420) of the cubic structure, which corresponded to diffraction angles of 32.09°, 11.44°, 65.88°, 72.14°, and 74.24°, respectively, according to JCPDS for ZnSe, and the results were in agreement with (Handique *et al*., 2023).We also observed the (100), (101), (102), and (002) values due to the hexagonal structure. After annealing the samples at 250 °C for 1 h, the intensity of all peaks increased, and another diffraction peak appeared at angles of 27.51°, 67.43°, 61.74°, and 53.63° at the (111), (112), (103), and 311 planes. A slight shift in the diffraction angles occurred, which is due to a slight displacement between adjacent multiple planes during the formation of double crystals. In addition, the heat treatment reduced the defect and increased the crystallinity of the ZnSe nanoparticles. The average crystal size decreased from 14.096 nm to 9.834 nm after annealing, which was calculated using the Scherrer eq. (2) (Chatterjee *et al*., 2014; Dhanam *et al*., 2008; Umme, 2010)

$$D = \frac{K\lambda}{\beta \cos\theta} \quad \text{----------(2)}$$

λ: wavelength equal (0.154 nm), β: width at half maximum and θ: Bragg's diffraction angle.

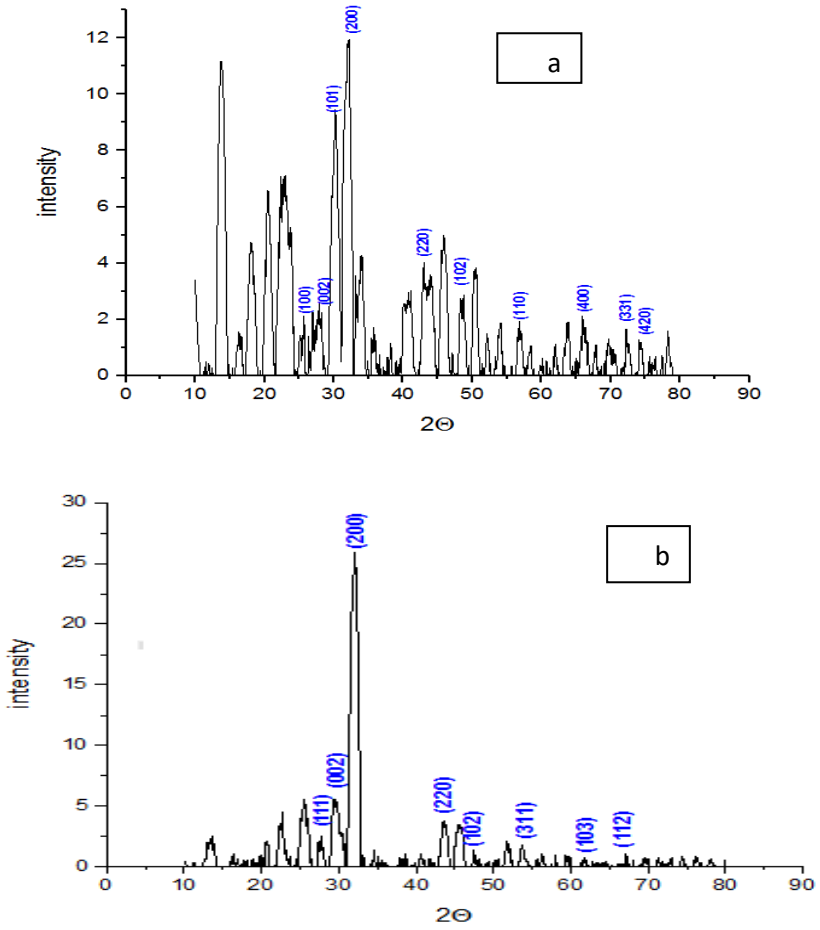

Fig. (4): XRD pattern for ZnSe (a) before annealing (b) after annealing

Table 1: Results XRD for ZnSe thin films before and after annealing

Samples	(hkl)	*2θ (deg.)*	d(Å)	FWHM	D/nm	Average crystal size/ nm
Before annealing	(100)	26.34746	3.35523	0.07330	19.308	14.096
	(002)	28.09165	3.12342	0.10000	14.287	
	(101)	30.36935	2.95603	0.17330	8.311	
	(200)	32.09302	2.79423	0.23270	6.198	
	(220)	44.11764	2.04960	0.24000	6.232	
	(102)	48.46785	1.88051	0.13330	11.407	
	(110)	56.81942	1.62809	0.06000	26.264	
	(400)	65.88919	1.42168	0.09330	17.703	
	(331)	72.14774	1.30783	0.10000	17.153	
	(420)	74.24076	1.27319	0.0000	--------	
After annealing	111))	27.51709	3.32161	0.13330	10.710	9.834
	(002)	29.52804	3.00720	0.00000	-------	
	200))	32.3671	2.76375	0.09330	15.468	
	(220)	43.56361	2.07551	0.20000	7.344	
	(102)	47.50342	1.91150	0.20000	7.573	
	(311)	53.63885	1.71309	0.15330	10.131	
	(103)	61.74418	1.49953	0.19330	8.354	
	(112)	67.4320	1.38774	0.18000	9.258	

In the (Fig. 5) the EDX spectral analysis of the Zinc selenide (ZnSe) sample shows the appearance of four peaks for the Zn element, located at (1,3 ,8., 9.5) keV and two peaks for the Se element, located at (11.1, 12.5) keV indicating the successful formation of the Zinc selenide (ZnSe) compound. We also note the presence of a sharp peak for the Si element, which is due to the composition of the glass substrate, as the film does not completely cover the substrate. The presence of other elements, such as C, O, Na, and Mg, indicates the presence of impurities during the preparation process (Sulaiman *et al*., 2025) which they have been shown in Table (2).

Table 2: Elemental atomic and weight percentage of ZnSe films by EDX analyses

Element	Atomic %	Atomic % Error	Weight %	Weight % Error
C	13.3	0.6	8.2	0.4
O	53.6	0.4	43.9	0.3
Na	10.1	0.5	11.9	0.6
Mg	1.0	0.1	1.2	0.1
Si	17.5	0.1	25.2	0.1
S	1.7	0.0	2.7	0.1
Cl	0.5	0.0	0.9	0.0
Ca	1.8	0.0	3.6	0.1
Zn	0.2	0.0	0.6	0.1
Se	0.4	0.0	1.8	0.2

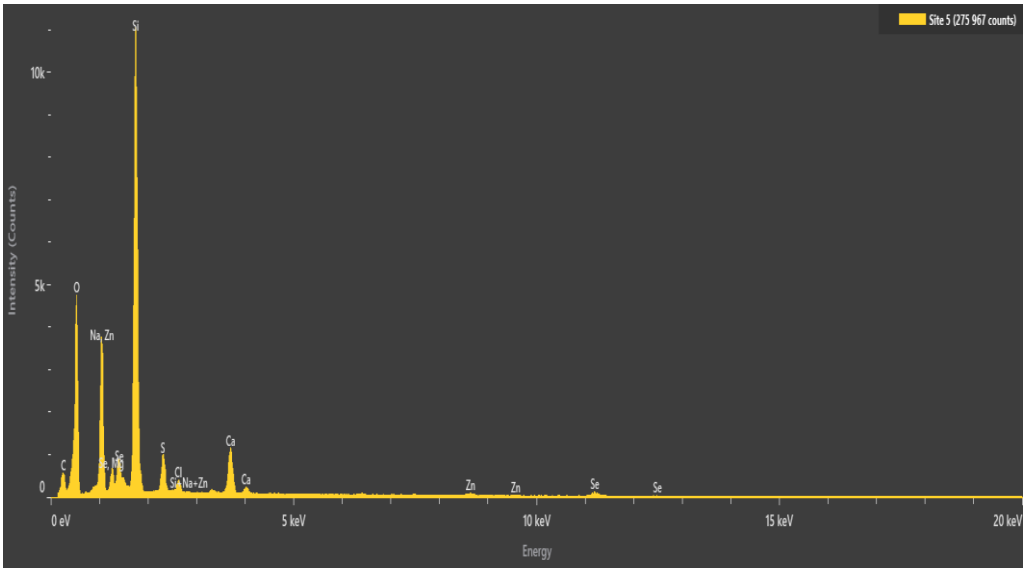

Fig. (5): EDXA of ZnSe nanoparticles prepared by CBD

Field emission scanning electron Microscope (SEM) device was used. The (Fig. 6) shows the SEM analysis of the sample at different magnifications (15,000X, 30,000X, 60,000X, 120,000X). We note that the shape of the particles is approaching a spherical shape with different sizes, with some scattered clusters and agglomerations and the appearance of cracks on the surface of the samples. Note that the background is smooth and flat, indicating the presence of a layer of precipitated ZnSe. As for the particles that appear at a magnification of 120,000X, the shape of the particles is spherical and of approximately the same size, distributed evenly over the surface of the sample, with sizes ranging between 21-35 nm, which is consistent with the sizes of ZnSe. (Toufanian *et al*., 2021).

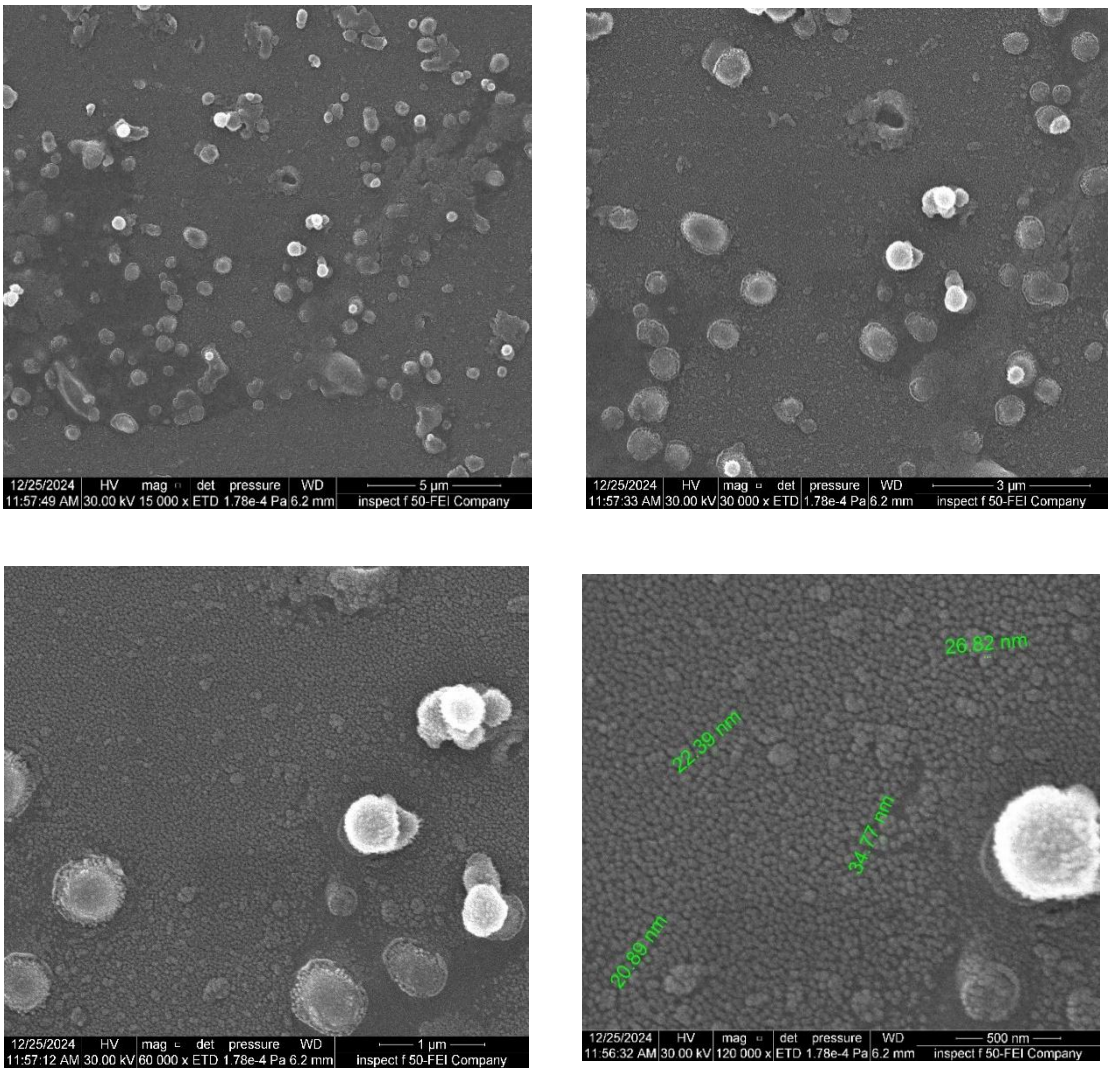

Fig. (6): FESEM image for ZnSe thin films syntheses at different magnification powers

CONCLOSIONS

In this paper, it is concluded that the transmittance of zinc selenide nanoparticles prepared by chemical bath deposition technique was exhibit the direct electronic transmission in the visible range at the wavelength range (400-780 nm). After annealing process at 250 °C for one hour, this value slightly increases in the same region. The optical study shows the presence of direct band gap. The band gap increases from 2.7 to 2.82 eV as the annealing temperature 250 °C in 1 h. XRD measurements indicate that the synthesized ZnSe and annealed films are in the cubic and hexagonal phase with a polycrystalline structure and the average crystal size for these films decreased from 14.096 nm to 9.834 nm respectively. EDX analysis shows the chemical composition of ZnSe films which indicates its successful formation. FESEM images of ZnSe films revealed that the particles were spherical and distributed randomly with diameters ranging from (21 to 35) nm.

REFERENCES

Abou El-Ela, I.; Abouda, A. A.; El-Sayed, M. E. M.; Younis, A. M. (2018). Effect of annealing on band gap and absorption in ZnSe thin films. *Opt. Mater.*, **86**, 66-72. doi.org/10.1016/j.optmat.2018.08.021

Chatterjee, U.; Das, A.; Ghosh, T.; Duttagupta, S. P.; Gandhi, M. N.; Singh, S. G. (2014). Effect of post deposition annealing on thermal evaporated ZnSe:Te towards a scintillator application. *Microel. Eng.*, **126**, 84-87. doi.org/10.1016/j.mee.2014.08.015

Chen, W.; Zhang, J. Z.; Joly, A. G. (2004). Optical properties and potential applications of doped semiconductor nanoparticles. *J. Nan. Nanot.*, 4(8), 919–947. doi.org/10.1166/jnn.2004.117

Deng, Z., Li; C., Liu, S.; Liu, Y. (2007). Preparation and size control of uniform ZnSe nanocrystals by a noninjection one-pot approach. *Nanot.*, **18**(28), 285608. doi.org/10.1088/0957-4484/18/28/285608

Dhanam, M.; Manoj, P. K. (2008). Properties of chemical bath deposited ZnSe thin films. *Mat. Chem. Phys.*, **109**(1), 59-65. doi.org/10.1016/j.matchemphys.2007.10.028

Elahi, M.; Shafiee, S. (2008). Study of structural and optical properties of ZnSe thin films grown by close spaced sublimation method. *Iranian Phys. J.*, **2**(4), 195-201.

Elsaeedy, H. I..; Hassan, A. A.; Yakout, H. A.; Qasem, A. (2021). The significant role of ZnSe layer thickness in optimizing the performance of ZnSe/CdTe solar cells for optoelectronic applications. *Opt. Laser Techn.*, **141**, 107139. doi.org/10.1016/j.optlastec.2021.107139

Ezema, F. I.; Osuji, R. U.; Ekwealor, A. B. C. (2007). Structural and optical properties of chemical bath deposited ZnSe thin films. *Chalc. Lett.*, **4**(11), 157–163.

Fang, X., Bando, Y.; Gautam, U. K. (2009). ZnS nanostructures: From synthesis to applications. *Adv. Mat.*, **21**(20), 2034-2054. doi.org/10.1002/adma.200802359

Gudiksen, M. S.; Lauhon, L. J.; Wang, J.; Smith, D. C.; Lieber, C. M. (2001). Growth of nanowire superlattice structures for nanoscale photonics and electronics. *J. Phy. Chem.B*, **105**(19), 4062-4064. doi.org/10.1021/jp004070f

Gupta, P.; Saxena, N. S.; Sharma, K.; Kumar, S. (2023). Optical and structural properties of nanocrystalline ZnSe thin films. *ACS. Omega*, **8**(5), 4870-4880. doi.org/10.1021/acsomega.2c07100

Handique, K. C.; Barman, B.; Kalita, P. K. (2023). Photo-response in chemically synthesized ZnSe nanorod for its application as photosensor. *Phys. Scr.*, **98**(11), 117001. doi.org/10.1088/1402-4896/acfea8

Kale, R. B.; Lokhande, C. D.; Mane, R. S. (2005). Structural, optical and electrical studies on ZnSe thin films deposited by chemical bath deposition method. *Semic. Sci. Techn.*, **20**(1), 1-5. doi.org/10.1088/0268-1242/20/1/001

Najim, S. A.; Jamil, N. Y.; Muhammed, K. M. (2019). Effect of au dopant on the structural and optical properties of zno thin films prepared by CVD. *J. Nano-Electr. Phys.*, **11**(2), 02003. doi.org/10.21272/jnep.11(2).02003

Prakash, D.; Singh, R. (2016). Structural and optical properties of ZnSe thin films prepared by thermal evaporation. *Mat. Res. Bull.*, **74**, 360–367. doi.org/10.1016/j.materresbull.2015.10.044

Rogach, A. L. (Ed.). (2008). "Semiconductor nanocrystal quantum dots: Synthesis, assembly, spectroscopy and applications". *Springer*. doi.org/10.1007/978-3-211-75237-1

Soonmin, H. (2023). ZnSe films: properties and applications. *Intern. J. Chem. Bioch. Sci.*, **24**(6), 307-319.

Sulaiman, A. A.; Aswad, T. A.; Karomi, I. B.; Najim, S. A. (2025). Pulse duration effect of laser ablation on the morphology properties of gold nanoparticles deposited on porous silicon. *J. Nano-Electr. Phys.*, **17**(2), 02015. doi.org/10.21272/jnep.17(2).02015

Toufanian, R., Salavati-Niasari, M.; Davar, F. (2021). Design and synthesis of ZnSe/CdTe nanocomposites for photovoltaic applications. *Chem. Mat.*, **33**(10), 3765-3773. doi.org/10.1021/acs.chemmater.1c00457

Umme, F.; Amina, R.; Tania, S. (2010). Study of ZnSe thin films for solar cell applications. *Sol. Energy Mat. Solar Cells*, **94**(9), 1571-1575. doi.org/10.1016/j.solmat.2010.05.015

Wang, C.;Wu, X.; Li, Y. (2005). Low-temperature synthesis of ZnSe nanowires and their optical properties. *Adv. Funct. Mater.*, **15**(9), 1503-1507. doi.org/10.1002/adfm.200500026

Wang, L.; Zhang, J.; Xu, J. (2010). Luminescence of ZnSe nanocrystals: Size effect and defect-related emissions. *J. Lumin.*, **130**(6), 1024-1028. doi.org/10.1016/j.jlumin.2010.01.020

تحضير جسيمات نانوية من سيلينيد الزنك باستخدام الترسيب بالحمام الكيميائي ودراسة طوبوغرافية السطح والخصائص البصرية

الاء عبد الخالق محمود **سهى عبد الله نجم**

جامعة الموصل/ كلية العلوم/ قسم الفيزياء

الملخص

في هذا البحث، وُجد أن نفاذية جسيمات نانوية من سلينيد الزنك المحضّرة بتقنية الترسيب في الحمام الكيميائي تُظهر انتقالًا إلكترونيًا مباشراً في المنطقة المرئية ضمن المدى الطيفي (400–780 نانومتر). وبعد إجراء عملية التلدين عند درجة حرارة 250 درجة مئوية لمدة ساعة واحدة، لوحظ حدوث زيادة طفيفة في قيمة النفاذية ضمن نفس المدى. أظهرت الدراسة البصرية وجود فجوة طاقة مباشرة، حيث ازدادت قيمة فجوة الطاقة من (2.7 إلى 2.82) إلكترون فولت عند التلدين بدرجة حرارة 250 °م لمدة ساعة. أشارت قياسات حيود الأشعة السينية (XRD) إلى أن الأغشية المحضّرة والمُلدّنة من ZnSe تتبلور في الطورين المكعّب والسداسي، وتتميز ببنية متعددة التبلور، كما لوحظ انخفاض في الحجم البلوري المتوسط من 14.096 نانومتر إلى 9.834 نانومتر على التوالي. أظهرت نتائج تحليل الطاقة المشتتة للأشعة السينية (EDX) أن التركيب الكيميائي لأغشية ZnSe يشير إلى تكوينها بنجاح. كما أظهرت صور المجهر الإلكتروني الماسح الميداني (FESEM) أن جسيمات أغشية ZnSe كانت كروية الشكل وموزعة بشكل عشوائي، بأقطار تتراوح ما بين (21 – 35) نانومتر.

الكلمات الدالة: غشاء رقيق، طوبوغرافية، بصرية، جسيمات نانوية، ZnSe.